IEEE Access
Multidisciplinary ⋮ Rapid Review ⋮ Open Access Journal

Received 2 August 2024, accepted 25 September 2024, date of publication 3 October 2024, date of current version 15 October 2024.

Digital Object Identifier 10.1109/ACCESS.2024.3473538

APPLIED RESEARCH

STPAS: Spatial–Temporal Filtering-Based Perception and Analysis System for Precision Aerial Spraying

JAEHWI SEOL[1,2], CHANGJO KIM[1,2], EUNJI JU[1], AND HYOUNG IL SON[1,2,3], (Senior Member, IEEE)

[1]Department of Convergence Biosystems Engineering, Chonnam National University, Buk-gu, Gwangju 61186, Republic of Korea
[2]Interdisciplinary Program in IT-Bio Convergence System, Chonnam National University, Buk-gu, Gwangju 61186, Republic of Korea
[3]Research Center for Biological Cybernetics, Chonnam National University, Buk-gu, Gwangju 61186, Republic of Korea

Corresponding author: Hyoung Il Son (hison@jnu.ac.kr)

This work was supported in part by the Regional Innovation Strategy (RIS) through the National Research Foundation of Korea (NRF) funded by the Ministry of Education (MOE) under Grant 2021RIS-002; and in part by the Cooperative Research Program for Agriculture Science and Technology Development, Rural Development Administration, Republic of Korea, under Project RS-2023-00232224.

ABSTRACT This study proposes a perception and analysis method for precise aerial spraying based on three-dimensional (3D) deep learning. Point cloud data for water droplets are acquired using 3D LiDAR, and the PointNet++ deep learning model is trained to classify and segment the spray pattern. Spatial-temporal data are processed for the segmented point cloud data. The spray from each nozzle is clustered through spatial data processing, and clustering is based on this information. This approach allows each nozzle to be distinguished and mapped. Processing temporal data compensates for unsensed or noisy data points and predicts the water droplet trajectories, enhancing the spray data. This method more accurately measures the shape of water droplets. Experiments altering the flight conditions of unmanned aerial vehicles (UAVs) were conducted to assess the proposed framework, demonstrating that processing is feasible in the onboard system of the UAV. The proposed method has potential application in control systems for precise spraying in the future.

INDEX TERMS Spatial-temporal filtering, clustering, grouping, precision aerial spraying.

I. INTRODUCTION

The agricultural paradigm has been shifting from traditional to digital agriculture due to the influence of the Fourth Industrial Revolution [1]. Precision agriculture is a prime example of digitalization in agriculture. In most cases of precision agriculture, intelligent and autonomous systems have been developed to improve crop quality and productivity [2], [3]. The agricultural task has been digitized using a variety of robots for various tasks such as monitoring [4], [5], crop counting [6], yield prediction [7], pest detection [8], [9], autonomous transporting [10], artificial pollination [11], and spraying [12].

Among various agricultural tasks, spraying consumes time and financial resources while profoundly affecting crop productivity and quality [13]. Existing methods have used speed sprayers on the ground to spray a significant volume of pesticide indiscriminately [14]. Such conventional spray methods have often led to adverse consequences, including alterations in soil properties from overusing pesticides, as many pesticides are applied without discrimination. Furthermore, these practices put farm workers at risk of pesticide exposure, potentially leading to poisoning [15].

Intelligent spraying systems have been studied to address this problem. Intelligent spray systems are based on unmanned ground vehicles to prevent pesticide exposure of farm workers. Subsequently, a system that selectively targets and sprays orchards based on crop recognition has been introduced to reduce soil contamination and economic loss due to pesticide overuse, leading to a more optimized intelligent spray system. However, ground-based spraying still encounters limitations such as overcoming large-scale

The associate editor coordinating the review of this manuscript and approving it for publication was Liandong Zhu.

environments, unstructured terrains, and other geographical constraints.

Research has shifted toward aerial spray control to address the limitations of ground-based spraying. Unmanned aerial vehicles (UAVs) have emerged as a promising platform for efficiently applying pesticides and fungicides, significantly contributing to the prevention and control of crop diseases and pests [16], [17]. Moreover, UAV-based spraying offers advantages in reducing the spray time and pesticide use [18]. However, the downward winds generated by UAV propellers pose a fundamental problem, hindering the effective delivery of pesticides to the intended target. Although UAV-based systems have enhanced efficiency by rapidly spraying chemicals, this increased efficiency has also heightened concerns about the potential drift of pesticide droplets into the environment. This problem arises during pesticide application across all platforms (ground and aerial), where drift can occur unintentionally during spraying, potentially causing damage to non-target crops. This problem must be carefully considered because it can precipitate serious consequences, including conflicts between farmers.

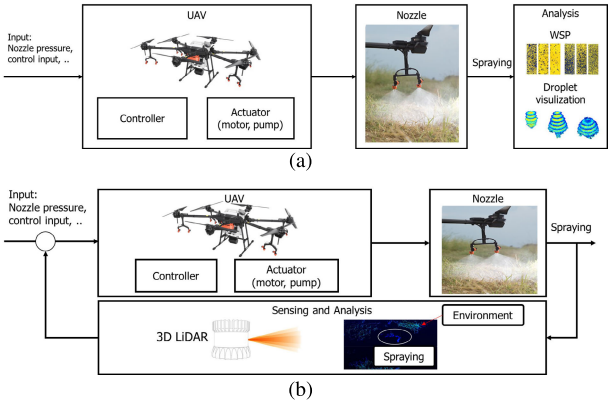

FIGURE 1. Spray control system (a) conventional (b) proposed (with feedback).

Previous research has revealed that 1% to 30% of sprayed pesticides can potentially drift into non-target areas [19]. Drift to non-target areas is unavoidable, necessitating the development of methods to reduce it. The development of intelligent and precise spray control systems could be a solution because they enable targeted and precise spraying. Similar to ground spraying, recognizing and targeting fruit trees is crucial, for intelligent aerial spraying. However, achieving precision in spraying is challenging from an aerial perspective due to the relatively lower resolution compared to images obtained from ground sprayers. Therefore, relying solely on fruit tree information for precise spraying becomes challenging. Consequently, a specific approach for aerial spraying is required. The first specific requirement is to measure the spray. Most previous research on measuring spray has focused on determining spray characteristics within specific settings and conditions. However, most of these studies have been conducted under static environmental conditions. In reality, natural environments are characterized by dynamic changes influenced by uncontrollable factors, such as wind direction and speed. Thus, research conducted under the assumption of controlling these variables makes it challenging to apply to real-world scenarios. Additionally, previous studies primarily focused on spatial data to identify and analyze spray characteristics. In this case, numerical simulations were developed using the spatial data of the spray to predict the spray. However, predictive models face challenges in obtaining accurate values for all variables and identifying the timing of drift occurrence without temporal information on spray over time. Therefore, new methods are needed to measure spray and analyze spray characteristics effectively in actual field conditions.

The second specific requirement is real-time control considering dynamic environment. For precise aerial spray control, a feedback control loop based on real-time measured spraying is necessary. However, previously researched spray models have been designed under constrained conditions such as assumptions regarding environmental variables and wind conditions, making them unsuitable for real-time control. Using pre-designed models for real-time control lacks consideration for environmental variables, resulting in incorrect spraying.

Currently, aerial spray control operates at the level depicted in Fig. 1(a), referencing spatial prediction models to control spraying by pre-defining the path and spray pressure. The approach in Fig. 1(a) depicts simple manual control through parameter settings. Therefore, to implement feedback control based on real-time data, as indicated in Fig. 1(b), spatial and temporal data on spraying must be measured in real-time.

This paper proposes a spatial-temporal filtering-based perception and analysis system (STPAS) for precise aerial spraying. The STPAS comprises real-time spray measurement coupled with spatial data filtering. Through this process, real-time spray characteristics can be obtained by quantitatively analyzing the results.

A. RELATED WORKS

1) SPRAY DETECTION

A study was conducted to recognize and characterize water droplets to determine the effectiveness of the water droplet spray system. Spray measurement methods can be categorized into two types: water-sensitive paper (WSP) analysis and spray shape visualization. This section outlines the existing spray measurement methods and reviews their limitations.

The WSP features a yellow surface with a special coating. Upon contact with water, the surface of the WSP changes color, turning blue when contacting water droplets. This characteristic is commonly studied to evaluate the spray pattern and degree of adhesion [20]. Specifically, this method has been employed to address the problem of unintentional spraying onto crops other than the intended target crop, primarily stemming from variations in spray coverage.

In another study [21], a pulse width modulation (PWM)-based spray system was designed to apply the necessary amount precisely where required. The characteristics of the spray were evaluated using a wooden structure attached to a WSP in the moving direction of the sprayer. In another study [22], the measurement of spray losses was determined using the WSP and nylon screens mounted at five heights on each of seven columns distributed at various distances. However, although this method can be effective in quantifying the spray, determining the characteristics of the spray is inherently challenging because this method relies solely on the spray adhering to the surface. Additionally, this method cannot analyze the result as a time series because it can only analyze data within that space.

Therefore, research was conducted to recognize sprays based on time-series data [23]. In these studies [24], [25], research was conducted based on computer vision and deep learning to detect and track the movement of water droplets captured by a camera. A portable visual sensor system was designed to detect the spray droplet deposition in UAV spray applications [26]. A learning model was designed by building a light adaptation model to consider the effect of light on image recognition. The droplet size range was investigated using optical diagnostic methods, including laser diffraction-based droplet sizing, high-speed photography, and microscopic flow visualization [18]. The spatial distribution of spray affected by crosswinds was investigated and measured using a two-dimensional patternator and WSP. However, the experiments were only performed in the laboratory or on a small scale and cannot be directly applied to actual applications. Afterward, a quantitative classification study was conducted by observing the spray drift using a mobile LiDAR method so that it could be applied in a real environment [27]. The drift analysis system was employed to cross-verify the performance of the developed intelligent spray system [13].

2) SPRAY ANALYSIS

Studies have been conducted to analyze droplet deposition and drift and the single or multiple independent factors that influence the deposition characteristics of water droplets sprayed by UAVs [28]. A study was conducted to determine the degree of deposition on the WSP to analyze the measured water droplets. In a study [29] images of the WSPs were analyzed using the fractal dimension, which was highly correlated with the quantitative spray measurements of the spray coverage and volume. This approach suggests the use of the fractal dimension as a quantitative measure to describe the regularity of the water droplets on the WSP.

Meteorological conditions, operating parameters, and the droplet size of the nebulizer affect the spray area and absorption adhesion to the target [28]. Therefore, single rotor-based aerial control was performed to determine the flight height, spray deposition (depending on the flight speed), number of spray depositions, coverage area, and droplet size [30]. Although the droplet parameter coefficients were determined from the experimental results, only water droplet data were still used. Moreover, [31] developed a computational fluid dynamics model to predict downwash within a tree canopy. A research method based on agricultural field environmental factors was proposed to simulate the deposition and drift characteristics of spray droplets numerically. Although a numerical analysis can help explain the effect of the applied parameters and tree structure on the distribution of the downdraft airflow within the tree canopy, it lacks reliability for field variables.

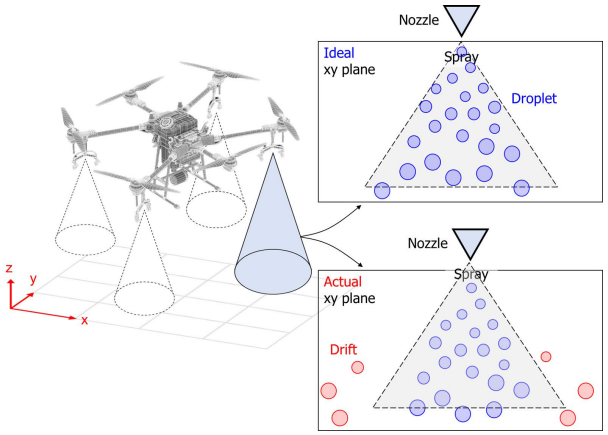

FIGURE 2. Illustration of the problem statement: The right top spray represents an ideal spray pattern according to the nozzle angle; The right bottom spray represents the actual spray pattern, which includes drift due to external forces.

3) SPRAY CONTROL

Existing methods have failed to spray target crops effectively because they maintain a consistent flow rate, resulting in problems that extend to the management of the surrounding areas. Therefore, research has recently been conducted to adjust the spray volume by considering the canopy variability [32]. In [33] found that droplet size was regulated to enhance the efficiency of the developed intelligent spray robot and mitigate the risk of unintended spraying. Droplet size was determined using PWM control, and the optimal PWM settings were identified by assessing the droplet size distribution, nozzle tip pressure, duty cycle, nozzle type, and gauge pressure.

Most of the related research has studied or developed ground spray robots. However, control methods for UAVs specifically designed for crop spraying have still not been reported. Compared to ground-based pesticide spray robots, UAV sprayers are significantly influenced by wind conditions inherent in aerial spraying, including downward winds. Therefore, precise spray in aerial spraying control systems is increasingly necessary.

B. CONTRIBUTIONS

The contributions and novelty of this study are summarized as follows:

1) Development of a perception system using a deep learning-based method in real-time.
2) Development of a process using spatial and temporal data processing to analyze the shape of the spray in real-time.
3) Field evaluation of the feasibility of implementation in real-world environments.

II. PROBLEM STATEMENT

As mentioned, the problem arising from the drift of insecticides for pesticide spray is depicted in Fig. 2. The desired outcome from aerial spray is ideally a straight-line distribution, as presented on the left. However, actual spraying, as depicted on the right, may result in some droplets being drift in unintended directions due to downdrafts generated by the UAV and natural winds present in the environment. This phenomenon must be accurately understood because it can lead to environmental and economic damage and pose health concerns. Thus, the spraying process must be sensed to address this problem.

This paper addresses the problem depicted in Fig. 3 concerning the challenges of sensing during spraying. When sensing the spray, there are instances where the sensors may fail to detect the spray due to their low resolution and the small size of the droplets. Additionally, with 3D LiDAR sensors operating at a sensing frequency of 10 Hz, sensing may be intermittent in some cases, as illustrated in the Fig. 3. Furthermore, the spraying process exceeds the detection range of the sensors in some instances. When intermittent detection occurs, droplets can be predicted through time-series data analysis. However, Exceeding the sensing range of the sensor presents clear limitations. In this study, exceeding the sensing range of droplets are assumed to have already occur drift.

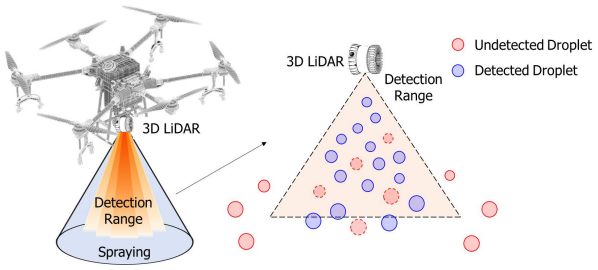

FIGURE 3. Water droplet sensing problem using three-dimensional LiDAR due to detection range (red circle) and low resolution (red dotted circle).

III. SPRAY PERCEPTION SYSTEM

For ideal aerial spraying, precise targeting is essential. Achieving accurate targeting requires considering the real-time variations in spray direction due to natural winds. The current methods, which rely on such techniques as the WSP or droplet collectors to understand spraying, can provide comprehensive data regarding the spatial distribution of the droplets. However, they have limitations in analyzing the variability of spraying, particularly concerning changes in direction or real-time movements (i.e., time-series data). Consequently, these existing methods cannot adjust spray techniques when the spray deviates from the intended target points due to the inability to pinpoint the exact moment when the spray is affected by the wind dynamics.

Therefore, in addition to the existing methods, time-series data must be incorporated into the analysis to enhance precision in aerial spraying. Hence, this paper proposes the STPAS to improve the accuracy of the aerial spraying control. The STPAS system is elaborated in Fig. 4, and for further details are presented in the STPAS flowchart in Fig. 5.

A. DETECTION

Accurate sensing methods are crucial for measuring spray patterns in precision aerial spraying. Traditionally, equipment used for environmental sensing includes radar or specialized devices explicitly designed for environmental monitoring [34]. However, such equipment lacks versatility and can be prohibitively expensive for integration into UAVs or real-time data monitoring. Therefore, this study use 3D LiDAR, which is commonly employed in autonomous driving. This decision is based on the considerations of price and real-time data communication for spray measurement under actual environmental conditions.

Short sensing intervals are necessary to detect natural environments and droplets swiftly, serving as a method to control UAVs, given the direct communication capability with the UAVs available in existing systems. Through this approach, a foundation is laid for real-time UAV control based on data obtained from 3D LiDAR. Although the accuracy of the sensor may not match that of sensors traditionally used in natural environments, the practicality of 3D LiDAR in real-world applications surpasses the limitations, even if it cannot provide precise measurements.

Operating at a sensing frequency of 10 Hz, 3D LiDAR recognizes the existence of all objects in a 3D space in each frame and represents them as points, forming a point cloud. Each sensed point contains 3D coordinates, intensity, and other information. Points are dependent on positional information; hence, they do not represent specific object sizes. This study focuses on identifying spray patterns; thus, a precise observation of droplet sizes is not necessary. Therefore, rather than observing droplet sizes accurately, the emphasis is placed on identifying the spray patterns.

B. SPATIAL DATA PROCESSING

In this stage, the process of handling the 3D point cloud of the spray based on the semantic segmentation PointNet++ [35] is explained to detect the spray pattern. The data obtained from the 3D LiDAR comprise point cloud data for all objects, including droplets. Therefore, it is necessary to separate the surrounding objects from the droplets. This paper employs the deep learning PointNet++ model (as shown in Fig. 6) to

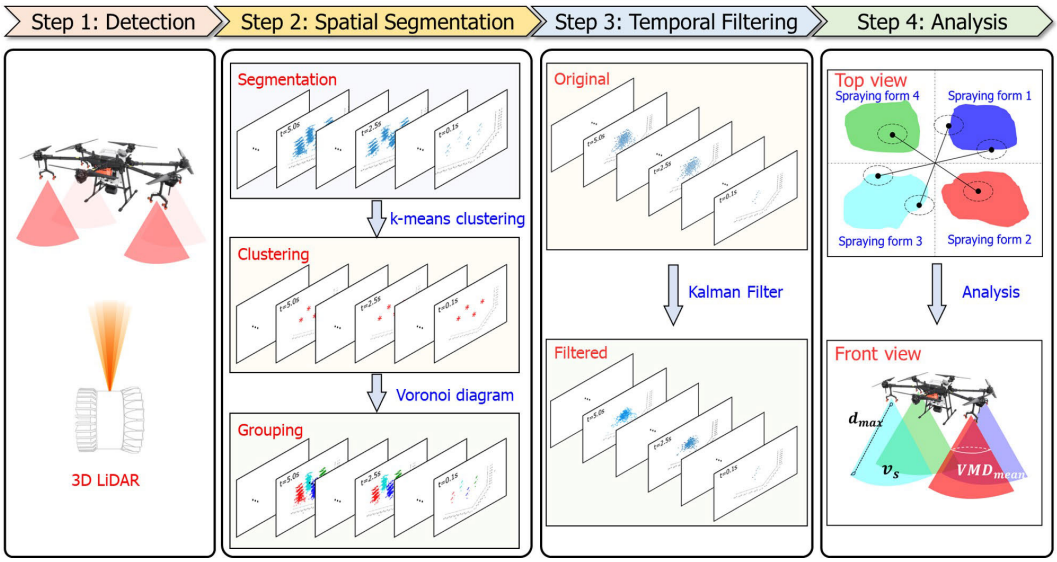

FIGURE 4. Steps in the spatial-temporal filtering-based perception and analysis system framework.

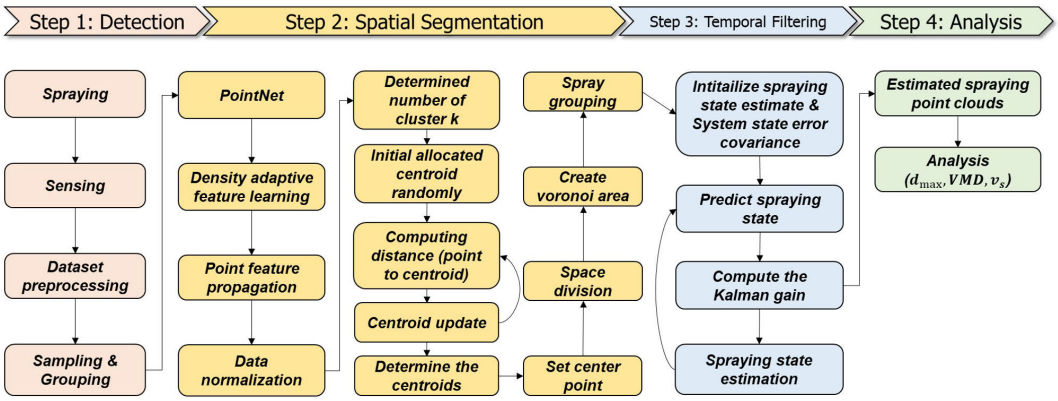

FIGURE 5. Flow chart of the spatial-temporal filtering-based perception and analysis system.

achieve this separation, for the detection and segmentation of droplets.

PointNet++ is a deep neural network algorithm that extends the hierarchical structure of PointNet for point cloud classification and segmentation tasks. The use of hierarchical structures allows for the gradual abstraction of larger local regions during exploration. Point cloud sets are successively reduced in size at each layer, obtaining more refined and abstract representations at each subsequent stage. These characteristics of PointNet++ facilitate the capture of detailed information, making it an ideal choice for analyzing spray patterns. Therefore, PointNet++ is employed as the learning model in this study.

Moreover, PointNet++ consists of two types of density adaptive layers: multi-scale grouping and multi-resolution grouping. The layer learns an optimized approach for merging multi-scale features by employing a random input dropout with a random probability for each instance. Owing to the multi-scale grouping operation of a local PointNet over a large neighborhood for every centroid, this method incurs significant computational expense. Two vectors are derived to address this problem: one by processing all raw points in the local region and another by selecting features from each sub-region at a lower abstraction level. Multi-resolution grouping is processed through a combination of two vectors, and this method is computationally more efficient because it circumvents feature extraction from large neighbors at the lowest level. This process accomplishes segmentation by extracting only the feature vectors of the spray.

1) SPRAY SEGMENTATION

First, the task of point cloud segmentation was formulated. The point clouds, denoted as P, contain n points $p_1, p_2, \ldots, p_n \in R^d$, with d-dimensional features. Each point p_1 comprises coordinates (x_i, y_i, z_i) in 3D space. The set of class labels is denoted as L. The segmentation of a point cloud

is the function f, which assigns a class to each point cloud P.

$$f : P \longmapsto \mathrm{L^n}. \tag{1}$$

This paper classifies spray from the point cloud, into two classes: UAV and spray. For segmentation, a training dataset was constructed in which the UAV and spray were labeled. Subsequently, pre-processed data were entered into PointNet++ for training, and semantic segmentation was performed. This approach improves the accuracy and efficiency of the spray data analysis with PointNet++.

The results derived from the learning model achieve semantic segmentation of the entire spray pattern. The spray pattern varies depending on the number and type of nozzles mounted on the UAV. The spray forms from each nozzle are different; hence, it is critical to differentiate each nozzle to sense and classify the spray form more accurately. Moreover, distinguishing each nozzle enables the possibility of individually controlling the nozzles on the UAV in the future. This paper proposes a method based on spatial data to segment the spray corresponding to each nozzle, aiming to distinguish the spray from each nozzle. The sections on clustering, grouping, and temporal filtering below provide detailed procedures for the classification task.

2) CLUSTERING

Spatial data processing was performed to distinguish the spray patterns emitted from each nozzle. Unlabeled points in space were classified using the k-means clustering algorithm. The k-means clustering algorithm is a well-known clustering method applied in data processing due to its simplicity in partitioning the collected data into k groups. With these characteristics, the k-means clustering algorithm can divide the data into k groups according to the number of nozzles, enabling differentiation and analysis of the characteristics of the spray emitted from each nozzle.

Moreover, k random clusters were generated to cluster the point cloud, classified as droplets. First, the number of clusters must be determined. The criterion for determining the number of clusters depends on the number and distribution of the nozzles on the UAV. In the UAV in this paper, spraying was conducted in four regions, with eight nozzles arranged in pairs of two. Consequently, for this paper, the number of clusters k was set to four. The clusters C are defined as follows:

$$C = \{c_1, c_2, c_3, c_4\}. \tag{2}$$

First, the initial centroids must be defined to achieve optimal clustering performance, which can be randomly set or manually selected. In this paper, the initial centroids were randomly set and generated, as depicted in Fig. 7. This approach is because UAVs always move dynamically during aerial spraying, making pre-specified cloud heads unreliable. Therefore, the initial centroids were randomly set and generated.

The cloud update process proceeds as follows. The sensed point clouds are assigned to the nearest of the randomly selected centroids. In this process, the distances between centroids and neighboring points are calculated using the Euclidean distance, and points are clustered to the closest centroid based on the calculated distances. The function for clustering is defined as follows:

$$J = \sum_{j=1}^{k} \sum_{i=1}^{n} min(\left\| p_i^{(j)} - p_j \right\|^2), \tag{3}$$

where n indicates the number of point cloud data, $p_i^{(j)}$ denotes each point cloud data, and p_j represents the centroid for cluster j. After allocating all provided data to the clusters, the centroid of each cluster was recalibrated to the average of the data points within that cluster. The clustering process, determined by the distance from the updated centroid and subsequent centroid updates, was repeated until convergence. Once this process was completed, the average nozzle positions were determined by the centroids. While the selected centroids provide information about the central points of the nozzles, additional processes are still required to analyze the spray patterns emitted from the nozzles.

3) GROUPING

The k-means clustering algorithm was employed to distinguish each nozzle in the spatial data, which involved initially generating k random centroids to cluster the point cloud. Grouping by clusters is required after completing the centroid generation process. The centroids generated using the k-means clustering algorithm were used for classification and visualization of the spray patterns emitted from the nozzles.

In this step, this approach performs grouping using Voronoi diagrams. Voronoi diagrams have a geometric structure that connects each point in space to the nearest point, adhering to the proximity rule [36]. Voronoi diagrams divide the entire space into k subspaces by describing which point in space is closest to a specific centroid for a given k. However, the traditional Voronoi diagram has primarily been employed to segment regions on a two-dimensional plane.

Aerial spraying occurs in 3D space; hence, the partitioning should consider the actual spray area. Therefore, a 3D space represented by $S = \{s_1, s_2, \ldots, s_k\}$ was defined, and the Voronoi diagram was extened into the 3D space. In this extension, the regions to be partitioned in the expanded space should not overlap. The non-overlapping 3D Voronoi diagram was established considering the sensing area of the Voronoi space. Subsequently, segments connecting the k centroids obtained from k-means clustering were created. Perpendicular bisecting planes were generated at the midpoints of these segments. These perpendicular bisecting planes were projected perpendicularly to the opposite direction of the reference point, and considering the sensing area, additional truncation was applied to the box portion, forming 3D Voronoi cells.

Formally, this can be expressed as follows. The set $P = \{p_1, p_2, p_3, \ldots\}$ is a set of n points in a space S. A 3D Voronoi diagram ($V(G)$) generated by the set P partitions S into k

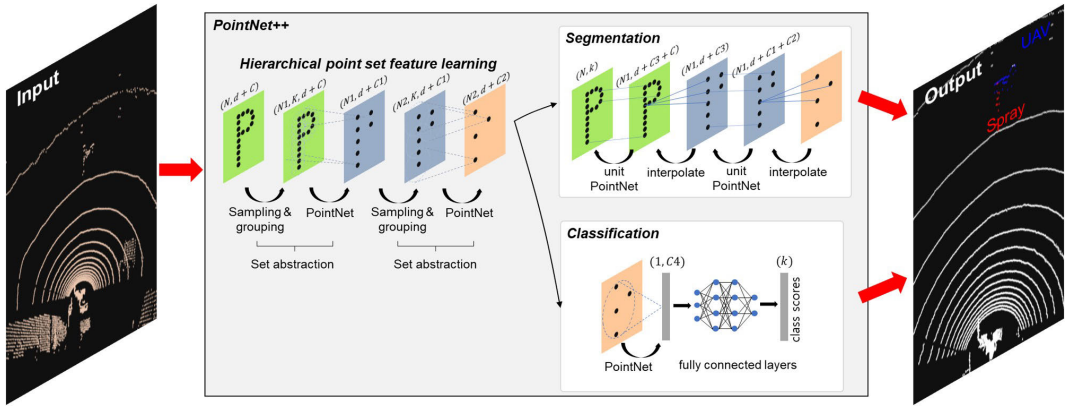

FIGURE 6. PointNet++ model based spray segmentation system architecture.

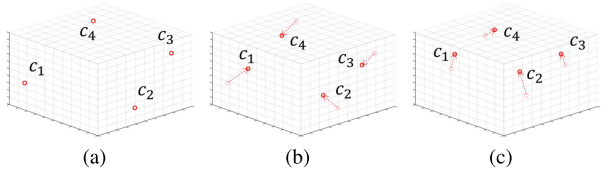

FIGURE 7. Centeriod update process of the *k*-means clustering algorithm by time variance: (a) $t = 0$ s, (b) $t = 2.5$ s, and (c) $t = 5$ s.

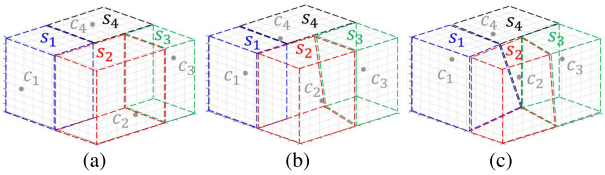

FIGURE 8. Voronoi diagram-based grouping algorithm results by time variance: (a) $t = 0$ s, (b) $t = 2.5$ s, and (c) $t = 5$ s.

regions. First, the centroid of the cluster and the divided space were calculated to divide the Voronoi space based on the Euclidean distance between a point q and centroid C as follows:

$$d(C, s_i) = \min_{c,q \in s_i} d(C, q), \tag{4}$$

where point q exists within the s_i space. The Voronoi space is defined as follows:

$$V(s_i) = \{s \in \mathbb{R}^3 | d(C, s_i) \leq d(C, s_j), \forall j \neq i\}, \tag{5}$$

where, the Voronoi diagram is $V(G) = \{V(s_1), \ldots, V(s_4)\}$. Based on the defined Voronoi diagram, the spray pattern is grouped at each nozzle, as illustrated in Fig. 8.

C. TEMPORAL FILTERING

Following the process described in the previous section, the set of points representing the spray was grouped based on spatial data. However, understanding aerial spraying in real-time requires consideration of time data. Therefore, this section explains the procedure for processing time-series data. In this step, time-series data compensate for measurement errors associated with 3D LiDAR. The measurement errors of 3D LiDAR, specifically those regarding the shape of the undetected droplets, are illustrated in Fig. 9. There may be cases where droplets exist outside the sensing range. Additionally, in some instances, droplets are within the sensing range but are temporarily undetected as shown in Fig. 9. For example, a droplet (p_1) may be captured at $t = 1$ but the same droplet (p_1') may not be detected at t = 1.1. Subsequently, at $t = 1.2$, the same droplet (p_1'') may suddenly be detected along the droplet trajectory. This occurrence indicates that, although still sprayed into the air, droplets may not be detected due to the low accuracy of the sensor. Therefore, a process to complement this is required.

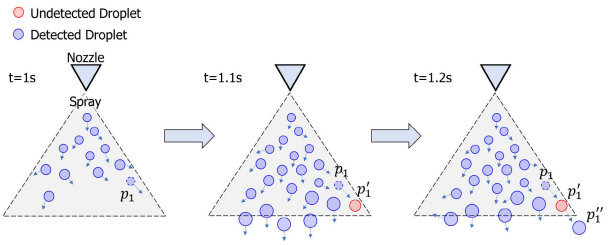

FIGURE 9. Problem of water droplets temporarily undetected within the detection range.

This paper implemented a filtering process based on the Kalman filter to solve the measurement error problem. The Kalman filter is used to estimate the state of a linear dynamic system based on measurements that contain noise. Therefore, it is suitable for such applications as aerial spraying where information from 3D LiDAR measurements may not be entirely accurate.

As depicted in Fig. 9, the trajectory of a specific water droplet can be predicted based on the previously measured p_1 and p_1'' using the Kalman filter. Then, the undetected droplet (p_1') can be compensated by predicted trajectory. Through this process, it is possible to compensate for

undetectable water droplets. The process of enhancing droplet tracking based on the Kalman filter is as follows.

The predicted ith point cloud of the spraying (s) at discrete time m is

$$\hat{s}_{m|m-1} = A\hat{s}_{m-1|m-1} + B_m u_m, \tag{6}$$

where $\hat{s}_{m|m-1}$ denotes the predicted spraying state, A is the state transition model, B_m represents the control input, and u_m indicates the control vector. The actual spray measurements from the 3D LiDAR sensor at m are as follows:

$$z_m = H_m\hat{s}_{m|m-1} + w_m, \tag{7}$$

where $H_m\hat{s}$ represents the observation operator, and w_m denotes the observation noise. The error covariance prediction is formulated as follows:

$$P_{m|m-1} = AP_{m-1|m-1}A^T + Q, \tag{8}$$

where Q represents the process noise covariance. The Kalman gain, which determines the weight assigned to the recent measurement, is as follows:

$$K_m = P_{m|m-1}H^T(HP_{m|m-1}H^T + R)^{-1}, \tag{9}$$

where R denotes the measurement noise covariance. Then, the state is updated as follows:

$$\hat{s}_{m|m} = \hat{s}_{m|m-1} + K_m(z_m - H\hat{s}_{m|m-1}), \tag{10}$$

Moreover, the updated error covariance is as follows:

$$P_{m|m} = P_{m|m-1} - K_m H P_{m|m-1}. \tag{11}$$

For all acquired point cloud data, the calculations are updated with system equations, and estimations are performed at specified intervals. A more accurate spray form can be achieved by predicting and estimating the point cloud for each previously classified nozzle.

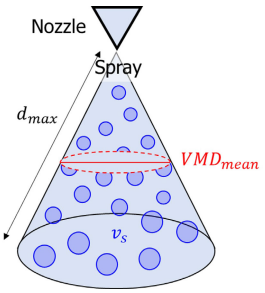

FIGURE 10. Performance measurement; a nozzle is evaluated by maximum distance (d_{max}), spray volume (v_s), and mean volume median diameter (VMD_{mean}).

IV. ANALYSIS

The evaluation metrics for STPAS are selected to analyze the spray pattern. In this process, analyzing the spray performance focuses on identifying the spray pattern and quantitatively evaluating it. The spray performance measurement is defined in Fig. 10. The spray trajectory emitted from the nozzle is determined by the type of nozzle. A flat-fan nozzle was employed in this work. Hence, the length of the lateral line of the cone and the circumference of the base of the cone are critical to reconstruct the shape. The lateral line length is obtained from the maximum spray distance, whereas the circumference of the base is estimated. The circumference of the base is obtained proportionally to the distance from the maximum distance to the central diameter, allowing the model to obtain a conical shape. The Performance metrics are defined as follows:

1) Maximum distance (d_{max}):

$$d_{max} = \left\| p_{close} - p_{far} \right\|^2, \tag{12}$$

where p_{close} denotes the closest point to the centroid, and p_{far} marks the farthest point from the centroid, enabling an assessment of the extent to which the spray was scattered. Analyzing the maximum spray distance in the hovering state using the calculated evaluation index provides valuable information, serving as a parameter guiding the UAV movement during precision aerial spray control or when adjusting the spray nozzle direction.

2) Spray volume (v_s):

$$v_s = \sum_{i}^{n} p_{spray.i}, \tag{13}$$

where p consists of spray point clouds. The spray volume is determined by the number of point clouds classified as p_{spray}, allowing an assessment of the quantity of scattered spray. Using the calculated evaluation index (assuming the UAV is hovering) enables the analysis of the current volume of spray released from the nozzle. Consequently, PWM control can be performed by adjusting the nozzle or pump mounted on the UAV. Notably, pertinent information can be extracted from each nozzle, serving as data for individually controlling the nozzles and pumping from the same nozzles mounted on the UAV.

3) Mean volume median diameter (VMD_{mean})

$$VMD_{mean} = \frac{1}{N}\sum(\alpha x + \beta y + \gamma z + \lambda), \tag{14}$$

where x, y, and z are determined based on the positions of the nozzle and UAV relative to the floor. A regression model was employed to represent the central diameter of the spray. The model was obtained through machine learning. In the formula, α, β, γ, and λ are distance-dependent coefficients determined through numerical experiments. These coefficients were empirically determined using data obtained while hovering at 3 m, with the corresponding parameters set to α is 15.38, β is 15.38, γ is -9.40, and λ is 158.22.

The VMD can be employed to estimate the 3D cone shape. First, the length of the side of the cone is obtained using the point cloud (i.e., centroid) closest to the nozzle location and the point cloud farthest away. Then, the 3D cone can be estimated using the central diameter of the cone through the VMD.

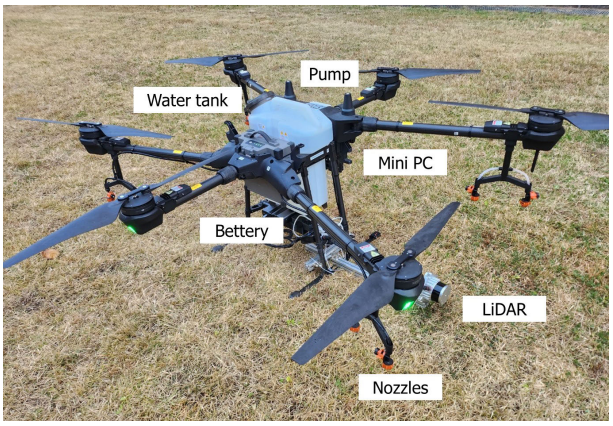

FIGURE 11. Aerial spray system with an embedded system capable of real-time recognition.

FIGURE 12. Capture of the experiment scene.

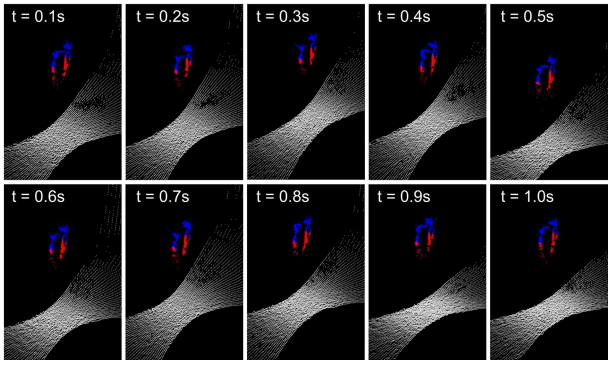

FIGURE 13. Capture of the experiment scene; red points represent a droplet, blue points represent a UAV, and white line represents a ground.

V. EXPERIMENT

A. EXPERIMENTAL SETUP

The aerial spray system is illustrated in Fig. 11. This study uses the Agras T16 model, equipped with eight nozzles. A 3D LiDAR sensor was mounted on a UAV to evaluate and analyze the spray pattern of the installed nozzles in this model. The UAV was equipped with a mini-computer, and the system was built so that all processing occurs onboard. The sensor placement was determined considering the detection range and operational conditions of the UAV, allowing it to detect the shape of the water droplets sprayed by the UAV in real-time.

However, placing the LiDAR at the central position to cover the entire area resulted in the loss of droplet detection in certain regions. Therefore, in this experiment, the 3D LiDAR sensor was strategically positioned closer to one side to ensure adequate coverage of a specific area while addressing the challenge of potential loss in the central region. Experiments were conducted using four nozzles on one side using this strategy.

The experiments were conducted to analyze the spray shape and characteristics in real-time according to the driving flight conditions of the UAV, as shown in Fig. 12, which were as follows:

1) Flight altitude (2 m, 3 m, and 4 m)
2) Flight velocity (1 m/s, 1.5 m/s, and 2 m/s)

According to the results [37], the maximum flight altitude should not exceed 2.5 m to minimize the drift of water droplets. Based on this result, the experimental conditions were determined by varying the driving conditions from 2 to 4 m. Additionally, the altitude was fixed at 3 m and the speeds were 1, 1.5, and 2 m/s.

B. EXPERIMENTAL RESULTS

The point cloud was segmented and classified into two classes. The overall accuracy, precision, and recall of the trained deep learning model were 99.4 %, 94.1 %, and 97.7 %, respectively. In addition, Fig. 13 depicts a snapshot of the real-time spray measurements taken during aerial spraying. The LiDAR sensor captures data at 10 Hz, enabling the monitoring and analysis of the spray pattern at 0.1-s intervals. As illustrated in Fig. 13, the evolving spray shape over time and the influence of the wind can be observed through the visualized data.

The spray measurement results are outlined according to the described method. Observing the initial unprocessed data state reveals numerous data oscillations over time, which are attributed to the calculation, including the noise in the unfiltered raw data, as depicted in Figs. 14-17(a). The graph, when filtered using the proposed method, is presented in Figs. 14-17(b). As depicted in Figs. 14 and 15(b), in the case of Nozzle 1, the maximum distance tends to increase with higher altitudes. The expansion of the maximum distance implies a broader spray range, posing challenges in achieving more precise spray control. Therefore, spraying at a lower altitude allows for more precise targeting. However, lower altitudes bring the UAV closer to the crops, potentially increasing the influence of downward wind on the crops, which could affect them. For Nozzle 2, no variation in height and velocity occurs, indicating that no distinct spray control is required, as illustrated in Figs. 14 and 15(b).

In the case of spray volume, Nozzle 1 tended to have a similar distribution regardless of the height, as depicted in Fig. 14(a), suggesting that the spray volumes are similar because the spray pressure does not change. However,

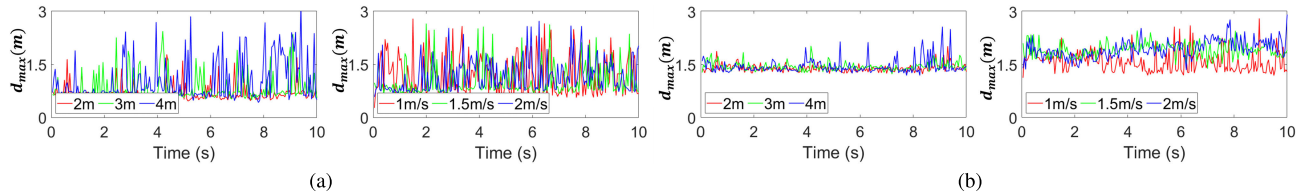

FIGURE 14. Experimental results for Nozzle 1: (a) original and (b) filtered maximum distance.

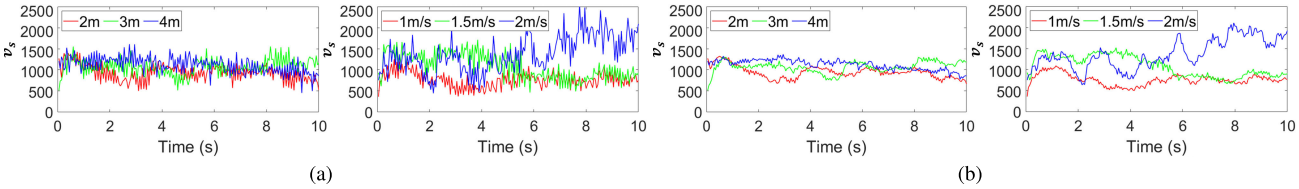

FIGURE 15. Experimental results for Nozzle 1: (a) original and (b) filtered spray volume.

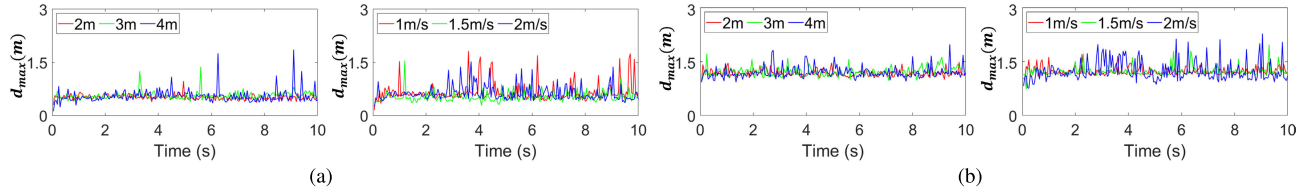

FIGURE 16. Experimental results for Nozzle 2: (a) original and (b) filtered maximum distance.

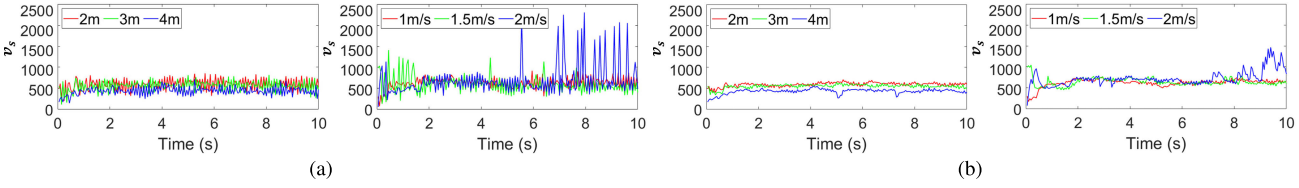

FIGURE 17. Experimental results for Nozzle 2: (a) original and (b) filtered spray volume.

for speed, the volume tended to increase as the speed increased, which may be because more spray was measured in conjunction with the sensing cycle, depending on the progress speed. Additionally, due to the influence of wind, water droplets sprayed from the surrounding nozzles may be included in the measurement. This phenomenon is not a measurement problem; however, it is a problem that can occur in actual applications. For Nozzle 2, a relatively minor change occurred in the height, however the speed displays a significant increase at 9 s, as indicated in Fig. 16(b). These results also suggest that the measured volume may be expected to increase due to the influence of wind, indicating a need for control in this case. No significant change occurred in the maximum distance, as depicted in Fig. 17(b).

These results enable real-time feedback control because they provide insight into the performance of each nozzle. The following section briefly discusses how the analysis results from the experiments can be used for real-time control. Additionally, the limitations of future precise aerial spray systems are presented, and additional solutions are proposed to ensure effective real-time control.

VI. DISCUSSION

This section discusses the primary challenge to consider for precise aerial spray control. More research and development have focused on ground spray systems than aerial spray systems, resulting in sufficient commercialization of ground-based spray platforms. The platforms for ground sprayers are standardized; thus research has been underway for ground spray systems on these platforms, with efforts to apply and integrate these systems. However, aerial spray systems have only recently begun to be applied in agriculture. The development of platforms for aerial sprayers has focused on improving location accuracy, autonomous control, and environmental sensing devices. Research on control systems for spray applications has been neglected, with more instances of simple tests being conducted using existing UAVs. Therefore, research on control systems that consider

real-time dynamic situations, environmental variables, and other factors is necessary.

Another problem is the insufficient explanation or selecting an appropriate nozzle based on the rotor downwash flow field in the literature, despite its importance in aerial spray systems [38]. Moreover, choosing anti-drift nozzles to achieve control over target crops may lead to decreased spray coverage. Therefore, the nozzle design is a crucial factor that facilitates spraying the target crop, and the trade-off between spraying performance and the reachability of the target crop must be managed effectively. Centrifugal nozzles have strengths in terms of spray volume and coverage area. However, wide spray coverage area may not be suitable for precise spraying methods. Because, to achieve a wide coverage, the increased number of water droplets sprayed from the nozzle reduces the straightness of droplets direction, thereby increasing the possibility of drift. Flat fan nozzles is reduced spray usage and improved linearity of spray moving direction, thereby decreasing the control complexity of precise spray systems. Furthermore, due to the lower spray volume compared to centrifugal separation nozzles, the risk of drift caused by wind may be reduced. Therefore, utilizing flat fan nozzles is expected to enable the establishment of a precise spray system.

VII. CONCLUSION

This study proposes a perception and analysis method for precise aerial spraying based on 3D deep learning. Point cloud data were acquired for water droplets using a 3D LiDAR sensor and deep learning models trained using PointNet++ to classify and segment the spray pattern. Spatial-temporal data processing was performed for the segmented point cloud data. The spray was clustered from each nozzle based on this information using spatial data processing, allowing each nozzle to be distinguished and mapped. Temporal data processing addressed the undetected or noise points and predicted the water-droplet trajectory to enhance the spray data. This approach more accurately measures the water droplet shape. Experiments were conducted to validate the proposed framework by altering UAV flight conditions, demonstrating the feasibility of the method for the UAV onboard system. This approach secures the potential application of the proposed method in control systems for precise spraying in the future.

REFERENCES

[1] C. Ju, J. Kim, J. Seol, and H. I. Son, "A review on multirobot systems in agriculture," *Comput. Electron. Agricult.*, vol. 202, Nov. 2022, Art. no. 107336.

[2] J. Jun, J. Kim, J. Seol, J. Kim, and H. I. Son, "Towards an efficient tomato harvesting robot: 3D perception, manipulation, and end-effector," *IEEE Access*, vol. 9, pp. 17631–17640, 2021.

[3] C. Ju and H. I. Son, "Modeling and control of heterogeneous agricultural field robots based on Ramadge–Wonham theory," *IEEE Robot. Autom. Lett.*, vol. 5, no. 1, pp. 48–55, Jan. 2020.

[4] T. Anand, S. Sinha, M. Mandal, V. Chamola, and F. R. Yu, "AgriSegNet: Deep aerial semantic segmentation framework for IoT-assisted precision agriculture," *IEEE Sensors J.*, vol. 21, no. 16, pp. 17581–17590, Aug. 2021.

[5] N. Rangappa, Y. R. V. Prasad, and S. R. Dubey, "LEDNet: Deep learning-based ground sensor data monitoring system," *IEEE Sensors J.*, vol. 22, no. 1, pp. 842–850, Jan. 2022.

[6] A. S. Gomez, E. Aptoula, S. Parsons, and P. Bosilj, "Deep regression versus detection for counting in robotic phenotyping," *IEEE Robot. Autom. Lett.*, vol. 6, no. 2, pp. 2902–2907, Apr. 2021.

[7] S. Sun, C. Li, A. H. Paterson, P. W. Chee, and J. S. Robertson, "Image processing algorithms for infield single cotton boll counting and yield prediction," *Comput. Electron. Agricult.*, vol. 166, Nov. 2019, Art. no. 104976.

[8] P. Temniranrat, K. Kiratiratanapruk, A. Kitvimonrat, W. Sinthupinyo, and S. Patarapuwadol, "A system for automatic rice disease detection from rice paddy images serviced via a Chatbot," *Comput. Electron. Agricult.*, vol. 185, Jun. 2021, Art. no. 106156.

[9] M. E. Bayrakdar, "A smart insect pest detection technique with qualified underground wireless sensor nodes for precision agriculture," *IEEE Sensors J.*, vol. 19, no. 22, pp. 10892–10897, Nov. 2019.

[10] J. Pak, J. Kim, Y. Park, and H. I. Son, "Field evaluation of path-planning algorithms for autonomous mobile robot in smart farms," *IEEE Access*, vol. 10, pp. 60253–60266, 2022.

[11] P. K. R. Maddikunta, S. Hakak, M. Alazab, S. Bhattacharya, T. R. Gadekallu, W. Z. Khan, and Q.-V. Pham, "Unmanned aerial vehicles in smart agriculture: Applications, requirements, and challenges," *IEEE Sensors J.*, vol. 21, no. 16, pp. 17608–17619, Aug. 2021.

[12] J. Seol, J. Kim, and H. I. Son, "Field evaluations of a deep learning-based intelligent spraying robot with flow control for pear orchards," *Precis. Agricult.*, vol. 23, no. 2, pp. 712–732, Apr. 2022.

[13] A. T. Meshram, A. V. Vanalkar, K. B. Kalambe, and A. M. Badar, "Pesticide spraying robot for precision agriculture: A categorical literature review and future trends," *J. Field Robot.*, vol. 39, no. 2, pp. 153–171, Mar. 2022.

[14] J. Kim, J. Seol, S. Lee, S.-W. Hong, and H. I. Son, "An intelligent spraying system with deep learning-based semantic segmentation of fruit trees in orchards," in *Proc. IEEE Int. Conf. Robot. Autom. (ICRA)*, May 2020, pp. 3923–3929.

[15] R. Berenstein and Y. Edan, "Automatic adjustable spraying device for site-specific agricultural application," *IEEE Trans. Autom. Sci. Eng.*, vol. 15, no. 2, pp. 641–650, Apr. 2018.

[16] C. Ju and H. I. Son, "Multiple UAV systems for agricultural applications: Control, implementation, and evaluation," *Electronics*, vol. 7, no. 9, p. 162, Aug. 2018.

[17] J. Kim, S. Kim, C. Ju, and H. I. Son, "Unmanned aerial vehicles in agriculture: A review of perspective of platform, control, and applications," *IEEE Access*, vol. 7, pp. 105100–105115, 2019.

[18] R. Alidoost Dafsari, S. Yu, Y. Choi, and J. Lee, "Effect of geometrical parameters of air-induction nozzles on droplet characteristics and behaviour," *Biosystems Eng.*, vol. 209, pp. 14–29, Sep. 2021.

[19] J. Perine, J. C. Anderson, G. R. Kruger, F. Abi-Akar, and J. Overmyer, "Effect of nozzle selection on deposition of thiamethoxam in Actara® spray drift and implications for off-field risk assessment," *Sci. Total Environ.*, vol. 772, Jun. 2021, Art. no. 144808.

[20] M. R. Bueno, J. P. A. R. D. Cunha, and D. G. de Santana, "Assessment of spray drift from pesticide applications in soybean crops," *Biosystems Eng.*, vol. 154, pp. 35–45, Feb. 2017.

[21] M. Grella, F. Gioelli, P. Marucco, I. Zwertvaegher, E. Mozzanini, N. Mylonas, D. Nuyttens, and P. Balsari, "Field assessment of a pulse width modulation (PWM) spray system applying different spray volumes: Duty cycle and forward speed effects on vines spray coverage," *Precis. Agricult.*, vol. 23, no. 1, pp. 219–252, Feb. 2022.

[22] R. Salcedo, H. Zhu, E. Ozkan, D. Falchieri, Z. Zhang, and Z. Wei, "Reducing ground and airborne drift losses in young apple orchards with PWM-controlled spray systems," *Comput. Electron. Agricult.*, vol. 189, Oct. 2021, Art. no. 106389.

[23] L. Li, R. Zhang, L. Chen, B. Liu, L. Zhang, Q. Tang, C. Ding, Z. Zhang, and A. J. Hewitt, "Spray drift evaluation with point clouds data of 3D LiDAR as a potential alternative to the sampling method," *Frontiers Plant Sci.*, vol. 13, Jul. 2022, Art. no. 939733.

[24] P. Acharya, T. Burgers, and K.-D. Nguyen, "AI-enabled droplet detection and tracking for agricultural spraying systems," *Comput. Electron. Agricult.*, vol. 202, Nov. 2022, Art. no. 107325.

[25] P. Acharya, T. Burgers, and K.-D. Nguyen, "A deep-learning framework for spray pattern segmentation and estimation in agricultural spraying systems," *Sci. Rep.*, vol. 13, no. 1, p. 7545, May 2023.

[26] L. Wang, W. Song, Y. Lan, H. Wang, X. Yue, X. Yin, E. Luo, B. Zhang, Y. Lu, and Y. Tang, "A smart droplet detection approach with vision sensing technique for agricultural aviation application," *IEEE Sensors J.*, vol. 21, no. 16, pp. 17508–17516, Aug. 2021.
[27] J. Seol, J. Kim, and H. I. Son, "Spray drift segmentation for intelligent spraying system using 3D point cloud deep learning framework," *IEEE Access*, vol. 10, pp. 77263–77271, 2022.
[28] Q. Weicai and C. Panyang, "Analysis of the research progress on the deposition and drift of spray droplets by plant protection UAVs," *Sci. Rep.*, vol. 13, no. 1, p. 14935, Sep. 2023.
[29] B. Brandoli, G. Spadon, T. Esau, P. Hennessy, A. C. P. L. Carvalho, S. Amer-Yahia, and J. F. Rodrigues-Jr, "DropLeaf: A precision farming smartphone tool for real-time quantification of pesticide application coverage," *Comput. Electron. Agricult.*, vol. 180, Jan. 2021, Art. no. 105906.
[30] F. Ahmad, B. Qiu, X. Dong, J. Ma, X. Huang, S. Ahmed, and F. Ali Chandio, "Effect of operational parameters of UAV sprayer on spray deposition pattern in target and off-target zones during outer field weed control application," *Comput. Electron. Agricult.*, vol. 172, May 2020, Art. no. 105350.
[31] H. Zhang, L. Qi, J. Wan, E. M. Musiu, J. Zhou, Z. Lu, and P. Wang, "Numerical simulation of downwash airflow distribution inside tree canopies of an apple orchard from a multirotor unmanned aerial vehicle (UAV) sprayer," *Comput. Electron. Agricult.*, vol. 195, Apr. 2022, Art. no. 106817.
[32] P. Berk, M. Hocevar, D. Stajnko, and A. Belsak, "Development of alternative plant protection product application techniques in orchards, based on measurement sensing systems: A review," *Comput. Electron. Agricult.*, vol. 124, pp. 273–288, Jun. 2016.
[33] T. R. Butts, L. E. Butts, J. D. Luck, B. K. Fritz, W. C. Hoffmann, and G. R. Kruger, "Droplet size and nozzle tip pressure from a pulse-width modulation sprayer," *Biosystems Eng.*, vol. 178, pp. 52–69, Feb. 2019.
[34] Z. Zhu, F. Yang, P. Kollias, R. A. Shaw, A. B. Kostinski, S. Krueger, K. Lamer, N. Allwayin, and M. Oue, "Detection of small drizzle droplets in a large cloud chamber using ultrahigh-resolution radar," *Atmos. Meas. Techn.*, vol. 17, no. 3, pp. 1133–1143, Feb. 2024.
[35] C. R. Qi, L. Yi, H. Su, and L. J. Guibas, "PointNet++: Deep hierarchical feature learning on point sets in a metric space," in *Proc. Adv. Neural Inf. Process. Syst.*, vol. 30, 2017, pp. 1–10.
[36] F. Aurenhammer, "Voronoi diagrams—A survey of a fundamental geometric data structure," *ACM Comput. Surveys*, vol. 23, no. 3, pp. 345–405, Sep. 1991.
[37] J. Wang, Y. Lan, H. Zhang, Y. Zhang, S. Wen, W. Yao, and J. Deng, "Drift and deposition of pesticide applied by UAV on pineapple plants under different meteorological conditions," *Int. J. Agricult. Biol. Eng.*, vol. 11, no. 6, pp. 5–12, 2018.
[38] P. Chen, J. P. Douzals, Y. Lan, E. Cotteux, X. Delpuech, G. Pouxviel, and Y. Zhan, "Characteristics of unmanned aerial spraying systems and related spray drift: A review," *Frontiers Plant Sci.*, vol. 13, Aug. 2022, Art. no. 870956.

JAEHWI SEOL received the B.S. and M.S. degrees from the Department of Rural and Biosystems Engineering, Chonnam National University, South Korea, in 2020 and 2023, respectively, where he is currently pursuing the Ph.D. degree with the Department of Convergence Biosystems Engineering. His research interests include field robotics, supervisory control, and discrete event systems.

CHANGJO KIM received the B.S. degree from the Department of Rural and Biosystems Engineering, Chonnam National University, Republic of Korea, in 2024, where he is currently pursuing the M.S. degree with the Department of Convergence Biosystems Engineering. His research interests include field robotics, multi-robot systems, harvesting robot, and agricultural robotics.

EUNJI JU is currently pursuing the B.S. degree with the Department of Convergence Biosystems Engineering, Chonnam National University, South Korea. Her research interests include autonomous control of UAV, field robotics, and agricultural robotics.

HYOUNG IL SON (Senior Member, IEEE) received the B.S. and M.S. degrees from the Department of Mechanical Engineering, Pusan National University, Republic of Korea, in 1998 and 2000, respectively, and the Ph.D. degree from the Department of Mechanical Engineering, Korea Advanced Institute of Science and Technology (KAIST), Republic of Korea, in 2010. In 2015, he joined as a Faculty Member of the Department of Convergence Biosystems Engineering, Chonnam National University, Gwangju, Republic of Korea, where he is currently a Professor. He is also affiliated as an Adjunct Professor with the Department of Robotics Engineering, Chonnam National University. Before joining Chonnam National University, from 2012 to 2015, he led the Telerobotics Group, Central Research Institute, Samsung Heavy Industries, Daejeon, Republic of Korea, as a Principal Researcher. He also had several appointments both academia and industry as a Senior Researcher with LG Electronics, Pyungtaek, Republic of Korea (2003–2005) and Samsung Electronics, Cheonan, Republic of Korea (2005–2009), a Research Associate with the Institute of Industrial Science, The University of Tokyo, Tokyo, Japan (2010), and a Research Scientist with the Max Planck Institute for Biological Cybernetics, Tübingen, Germany (2010–2012). His research interests include field robotics, hybrid systems, haptics, teleoperation, and agricultural robotics.